

A new mindlin FG plate model incorporating microstructure and surface energy effects

F.F. Mahmoud^a and M. Shaat^{*}

Mechanical Engineering Department, Zagazig University, Zagazig 44511, Egypt

(Received June 30, 2014, Revised September 12, 2014, Accepted October 2, 2014)

Abstract. In this paper, the classical continuum mechanics is adopted and modified to be consistent with the unique behavior of micro/nano solids. At first, some kinematical principles are discussed to illustrate the effect of the discrete nature of the microstructure of micro/nano solids. The fundamental equations and relations of the modified couple stress theory are derived to illustrate the microstructural effects on nanostructures. Moreover, the effect of the material surface energy is incorporated into the modified continuum theory. Due to the reduced coordination of the surface atoms a residual stress field, namely surface pre-tension, is generated in the bulk structure of the continuum. The essential kinematical and kinetically relations of nano-continua are derived and discussed. These essential relations are used to derive a size-dependent model for Mindlin functionally graded (FG) nano-plates. An analytical solution is derived to show the feasibility of the proposed size-dependent model. A parametric study is provided to express the effect of surface parameters and the effect of the microstructure couple stress on the bending behavior of a simply supported FG nano plate.

Keywords: couple stress theory; nanomechanics; nano plates; functionally graded materials; surface elasticity; size-dependent model

1. Introduction

Classical continuum mechanics of solids is based on the assumption that matter is continuously distributed throughout the solid. This classical theory disregarded the molecular structure of matter and neglected the microstructure size-dependency which causes the physical breakdowns of classical continuum mechanics in micro/nano scale applications. The challenge is to adopt the classical continuum theories to account for the size dependency and the discrete nature effect of the material microstructure, keeping the continuity assumptions and considerations.

Interactions at microscopic scale are the physical origin of many macroscopic phenomena. In conventional theories of continuum mechanics, a material body is modeled as a continuum consisting of an infinite number of material particles. Each material particle is treated as a mass point. However, in the microcontinuum theories, the microstructure of the material particle must be considered to describe the microscopic motion and to account for the microstructure size-

^{*}Corresponding author, Ph.D. Student, E-mail: ShaatScience@yahoo.com

^aProfessor, E-mail: faheem@aucegypt.edu

dependency. Chen *et al.* (2004) provided an atomistic viewpoint of the applicability of microcontinuum theories. First established; in Micromorphic theory (Eringen and Suhubi 1964, Eringen 1999) a material body is a continuous collection of a relatively large number of deformable particles, with each particle possessing finite size and inner structure. The Micromorphic theory is based basically on the kinetics and interactions of atoms where the deformation involves macro-strains (displacement gradients of the center of the particles) and microscopic internal strains (microscopic internal displacement gradients within the structure of the particle). The microstructure of the particle in Micromorphic theory consists of a finite number of unit cells.

For infinitesimal deformation and slow motion assumptions, the Micromorphic theory is reduced to Microstructure theory, Mindlin (1964), where the kinetics of atoms are ignored. In Micropolar theory, Eringen and Suhubi (1964), the material particle is considered as rigid, i.e., neglecting the internal possible motions within the inner structure of the particle. It accounts for the atomic dynamic effect for materials with stiff, nearly rigid, microstructures.

When the deformation of the microstructure of the particle is very small and the change of the orientation can be ignored, the Micropolar theory can be reduced to Cosserat theory (Cosserat and Cosserat 1909) which is not suited for problems involving the significant change of the orientation of the microstructure. In the original Cosserat theory, the kinematical quantities were the displacement and a material microrotation, which is assumed to be independent of the continuum macrorotation.

In the classical couple stress theory (Mindlin and Tiersten 1962, Toupin 1962), the distinction of macromotion of the particle and the micromotion within its structure is eliminated. The couple stress theory, by including higher order stress measure, provides a suitable size-dependent model for microscopically homogenous materials that possess only one atom per crystal in the unit cell.

Nonlocal theory (Eringen 1966, Edelen 1969) considers the long-range interatomic interactions and yields size-dependent results. The effect of microstructure does not appear in the theory where the particle is idealized as a mass point, similar to the classical continuum theory. The Nonlocal theory can be applied to a crystal that has only one atom per the unit cell at various length scales.

Here in this paper, the effects of microscopic interactions on the continuum mechanics in the frame work of the modified couple stress theory are considered for linear elastic materials. In classical couple stress theories (Mindlin and Tiersten 1962, Toupin 1962, Koiter 1964), the applied loads on the material particle include not only a force to drive the material particle to translate but also a couple (of forces) to drive it to rotate. In this classical conception, only the conventional equilibrium relationships of forces and moments (of forces) are enforced and the couple is unconstrained in the absence of higher order equilibrium requirements. The modified couple stress theory proposed by Yang *et al.* (2002) results from the classical couple stress theory to introduce only one material length scale and to include a symmetric couple stress tensor to be consistent with higher order theories.

Based on the modified couple stress theory, several size-dependent beam and plate models have been developed to capture the size effects in small scale structures. For example, Park and Gao (2006) developed an Euler-Bernoulli beam model for bending analysis of nanobeams. This model was employed by Kong *et al.* (2008), Kahrobaiyan *et al.* (2010) to study vibration of microbeams. Ma *et al.* (2008) developed a Timoshenko beam model to incorporate the effects of transverse shear deformation and rotary inertia. The Timoshenko beam model was adopted to study the buckling (Fu and Zhang 2010) and vibration (Ke and Wang 2011, Ke *et al.* 2011) of microtubes. Tsiatas (2009) first developed a Kirchhoff plate model for static analysis of microplates. This

model was used by Yin *et al.* (2010), Jomehzadeh *et al.* (2011) to study the vibration of microplates. To account for the effects of transverse shear deformation and rotary inertia in moderately thick microplates, Ma *et al.* (2011), Ke *et al.* (2012) developed a Mindlin plate model. Recently, Thai and Choi (2013) proposed a size-dependent FG Kirchhoff and Mindlin plate models based on the modified couple stress theory. They provided analytical solutions to study the bending, buckling and vibration of FG nano-plates. Arbind and Reddy (2013) proposed the nonlinear analysis of FG beams with account for the microstructural length scale and the Von Karman nonlinearity.

Another physical reason for the breakdown of classical continuum mechanics at micro/nano-scale sizes is surface energy effects. Atoms at or near a free surface experience reduced coordination, due to a different local binding environment, than the interior atoms. As a consequence of under-coordination, the surface will be subjected to a residual stress, namely surface tension. In order to keep equilibrium, a residual stress field in the bulk will be induced by surface tension in the reference configuration that is not subjected to any external loading (Ru 2010, Shaat *et al.* 2013a, Wang and Zhao 2009). For the induced residual stresses in elastic continua due to inclusion of surface tension in the framework of continuum thermodynamics, the reader could refer to Wang and Zhao (2011). Such surface effects are negligible in macro-scale sizes of solids; however, in micro/nano-scale sizes such effects will be significant. Gurtin and Murdoch (1975, 1978) adopted the classical continuum theory and formulated a surface elasticity model, where the surface of solids can be viewed as a 2D elastic membrane with different material constants (due to environmental interactions) adhering to the underlying bulk material without slipping. Recently, many researchers have studied the effect of surface energy on the elastic behavior of nano-structural elements based on Gurtin and Murdoch surface model (Lu *et al.* 2006, Shaat *et al.* 2012, 2013b, c, Lü *et al.* 2009, Wang *et al.* 2010). In Gurtin and Murdoch model, the surface is represented as a single layer consisting of an infinite number of material particles as in classical elasticity, neglecting the microstructure of the surface. However, Guo and Zhao (2005, 2007) considered the microstructure of the surface of nanofilms and nanobeams, where the surface consists of multi-layers of relaxed crystals. A lattice model is proposed where the possible bond relaxation of the atom is considered which alter the mechanical properties of the nano film. This issue could be considered in another work.

Functionally graded materials (FGMs) are microscopically inhomogeneous composite materials, in which the volume fraction of the consistent materials is varied continuously as a continuous function of the material position along one or more dimension of the structure. Recently, FGMs have attracted much attention due to their effectiveness for various applications such as thermal coatings of barrier for ceramic engines, gas turbines, nuclear fusions, optical thin layers, biomaterial electronics, etc. Therefore, many researchers have studied the thermo-mechanical behavior of FGMs in different situations (Alieldin *et al.* 2011, Alshorbagy *et al.* 2013, Alibeigloo 2010).

Due to their versatility of behavior, FGMs are now widely used in nanoscale applications such as nano-optoelectronic and nano-thermoelectric materials (Bharti *et al.* 2013). The carbon nanotubes reinforced functionally graded composite materials are expected to be the new generation material having a wide range of unexplored potential applications in various technological areas such as aerospace, energy, automobile, medicine, structural and chemical industry. They can be used as gas adsorbents, templates, actuators, catalyst supports, probes, chemical sensors, nanopipes, nano-reactors etc. To this aim scientists exerted their efforts to propose innovative technologies to fabricate, with fewer prices, FGMs for nanoscale applications

(Bafekrpour *et al.* 2012, Birman and Byrd 2007).

In plate theory, the neutral plane is coincident with the geometric mid-plane of isotropic plates. However, the neutral plane of FG plates may not coincide with their geometric mid-plane, because of the material property variation through the plate thickness. It had been approved that the neutral plane position plays an important role in studying the bending behaviors of FG plates; therefore the position of the neutral plane for FG plates must be predetermined (Shaat *et al.* 2013b, c). Yaghoobi and Fereidoon (2010) studied the influence of neutral plane position on deflection of FG beams under uniformly distributed load.

Unfortunately, all above mentioned studies dealt separately with the effect of surface energy or the effect of couple stress on nano structures. However, it is convenient to consider both surface and microstructure effects, altogether, in studying the behavior of nanosolids. Recently, Gao and Mahmoud (2014), Mahmoud *et al.* (2012) considered both the microstructure effect in combining with surface energy effect on bending behavior of nano beams. Moreover in our previous work (Shaat *et al.* 2014), effects of both of surface and microstructure, in the context of the modified couple stress theory, are considered in studying the bending behavior of Kirchhoff nano plates. Here in this paper, the bending behavior of FG ultra-thin Mindlin plates is investigated considering both the microstructure effects, in the context of the modified couple stress theory, and surface energy effects. The fundamental equations and relations for the modified couple stress theory are derived to illustrate the microstructural couple stress effects on nanosolids. Moreover, the effect of the material surface free energy is incorporated into the modified continuum theory. The essential kinematical and kinetically relations for nano-continuum mechanics of nanosolids are derived and discussed. Then, based on the modified couple stress theory, these essential relations are used to derive the size-dependent Mindlin model for ultra-thin FG films considering the exact neutral plane position. In order to illustrate the microstructure couple stress and the surface energy effects, an analytical solution is derived and used to provide a parametric study.

2. Modified couple stress theory

2.1 Kinematics

Here the kinematics of a continuum under the assumptions of infinitesimal deformation is presented. Deformation of a continuum refers to relative displacements and changes in the geometry experienced by the continuum under the influence of a force system. To well represent the induced deformations in a continuum, consider a fiber element ($d\mathbf{X}$) connects two material particles P_0 and Q_0 in the reference configuration (see Fig. 1). In the deformed configuration, the two material particles take up positions P_4 and Q_4 , due to successive sequences of induced changes in the fiber element ($d\mathbf{X} \rightarrow d\mathbf{x}_4$).

The displacement gradient tensor and the gradient rotation tensor at particle P_0 which represent the relative displacement and rotation gradients of particle Q_0 with respect to P_0 are

$$u_{i,j} = \varepsilon_{ij} + \theta_{ij} \quad ; \quad \theta_{i,j} = \chi_{ij} + k_{ij} \quad (1)$$

where the displacement gradient tensor $u_{i,j}$ and the rotation gradient tensor $\theta_{i,j}$ are decomposed into their symmetric and skew-symmetric parts.

In classical continuum mechanics only the displacement gradient tensor is considered to illustrate the possible deformations of the fiber element. With

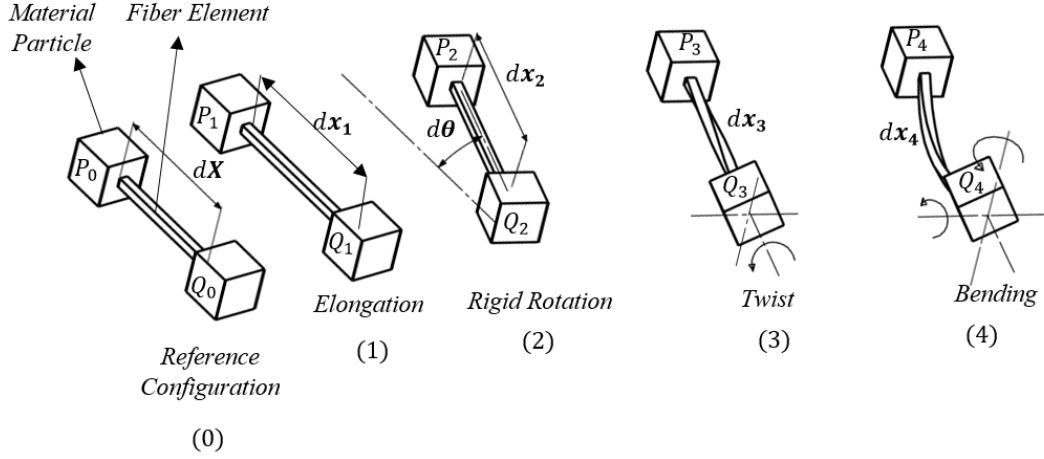


Fig. 1 A fiber element $d\mathbf{X}$ between two material particles P_0 and Q_0 and the successive sequences of induced changes in the fiber element. (0) the reference configuration (1) possible stretches in the fiber element (2) rigid-like rotation of the fiber element (3) possible twist induced in the fiber element (4) possible bending induced in the fiber element.

$$\varepsilon_{ij} = \frac{1}{2}(u_{i,j} + u_{j,i}) \text{ and } \theta_{ij} = \frac{1}{2}(u_{i,j} - u_{j,i}) \tag{2}$$

where ε_{ij} is the symmetric infinitesimal strain tensor (small deformation tensor) which is the suitable measure of deformation induced in the fiber element that contribute to elongation or contraction in the fiber element ($d\mathbf{X} \rightarrow d\mathbf{x}_1$ in Fig. 1). While θ_{ij} is the skew-symmetric infinitesimal rotation tensor which measures the rigid-like rotations of the fiber element between the two material particles ($d\mathbf{x}_1 \rightarrow d\mathbf{x}_2$ in Fig. 1). We have to note that, θ_{ij} does not contribute to the change in the fiber element length and consequently cannot appear in a tensor measuring material deformations. As a result, in classical continuum theories, such as Cauchy elasticity, such rotation tensor is disregarded and ε_{ij} is used as a measure of the induced deformation in the continuum (Hadjefandiari and Dargush 2011).

However, in nano-size continuums, in addition to the contribution of the stretches of the fiber element, it is convenient to have an additional tensor measures the possible twisting and bending of the fiber element, which come as a consequence of the possible relative rotations of the two material particles P_0 and Q_0 . Consequently, in the couple stress theory, we expect to include the curvature tensor $\theta_{i,j}$ which is the gradient of the rotation vector ($\theta_i = \frac{1}{2}e_{ijk}\theta_{kj}$) at particle P_0 . The diagonal components of the $\theta_{i,j}$ tensor represent the pure torsion of the fiber element while the off-diagonal components represent the total curvatures-due-to-bending of the fiber element.

The rotation gradient tensor $\theta_{i,j}$ could be decomposed into χ_{ij} and k_{ij} with

$$\chi_{ij} = \frac{1}{2}(\theta_{i,j} + \theta_{j,i}) ; k_{ij} = \frac{1}{2}(\theta_{i,j} - \theta_{j,i}) \tag{3}$$

The diagonal components in the symmetric tensor χ_{ij} represent the pure torsion of the fiber element ($d\mathbf{x}_2 \rightarrow d\mathbf{x}_3$ in Fig. 1) while the off-diagonal components measure part of the curvatures-due to-bending of the fiber element ($d\mathbf{x}_3 \rightarrow d\mathbf{x}_4$ in Fig. 1). On the other hand, the skew-symmetric

tensor k_{ij} measures the other part of the curvatures-due-to-bending of the fiber element ($d\mathbf{x}_3 \rightarrow d\mathbf{x}_4$ in Fig. 1). The latter, k_{ij} , has zero diagonal components, while the off-diagonal components represent the mean curvatures of the fiber element. These two tensors account for the deformation energy of the fiber element, in addition to the conventional infinitesimal strain tensor ε_{ij} .

By discussing some kinetic concepts of the mechanics of particles, Yang *et al.* (2002) provided a third higher order equilibrium equation in addition to the conventional equilibrium equations of material particles. This third additional equation requires that summation of couples of couples at the level of material particles to be zero to achieve equilibrium. Consequently, to successfully apply the third proposed equation the skew-symmetric couple stress tensor has to be eliminated. This theory is based on that the couple stress is not a free vector but a local driving force that rotates the material particles in addition to the conventional affected forces. This modifies the classical couple stress theory to be consistent with higher order theories of solid mechanics. Consequently, we could conclude that, in the modified couple stress theory, the deformation of the continuum depends only on the symmetric part of the displacement gradient tensor (symmetric infinitesimal strain tensor) (ε_{ij}) and the symmetric part of the rotation gradient tensor (χ_{ij}).

2.2 Strain energy density function and constitutive equations

In this paper, the continuum microstructure is modeled based on the modified couple stress theory in which the strain energy is a function of the infinitesimal strain ε_{ij} in addition to the symmetric rotation gradient tensor χ_{ij} and can be expressed as follows (Yang *et al.* 2002).

$$W = W(\varepsilon_{ij}, \chi_{ij}) = \frac{1}{2} \lambda \varepsilon_{ii} \varepsilon_{jj} + \mu \varepsilon_{ij} \varepsilon_{ij} + \mu \ell^2 \chi_{ij} \chi_{ij} \quad (4)$$

Consequently, the constitutive equations for the modified couple stress theory are

$$\sigma_{ji} = \frac{\partial W}{\partial \varepsilon_{ij}} = \lambda \varepsilon_{pp} \delta_{ij} + 2\mu \varepsilon_{ij} \quad (5a)$$

$$m_{ji} = \frac{\partial W}{\partial \chi_{ij}} = 2\mu \ell^2 \chi_{ij} \quad (5b)$$

where λ and μ are continuum bulk Lamé constants and ℓ is a material length scale parameter which is regarded as a material property measuring the effect of couple stress. This parameter can be determined from torsion tests of slim cylinders (Chong *et al.* 2001) or bending tests of thin beams (Lam *et al.* 2003). σ_{ji} and m_{ji} are the force-stress tensor and the couple-stress tensor, respectively. These two tensors are symmetrical ones.

3. Surface elasticity theory

In the presence of initial surface tension, the surface of an elastic body does not have a “natural state” characterized by zero surface energy. Moreover in the presence of initial surface tension, the theory of surface elasticity is a hybrid formulation characterized by linearized bulk elastic material and second order finite deformation of the surface (Ru 2010, Shaat *et al.* 2013a).

For classical linear elasticity, it is not necessary to distinguish the initial/deformed areas, because this only causes high-order infinitesimal terms which are discarded in linear elasticity. For surface elasticity, however, because of the pre-existing surface tension, the finite change in surface

area should be accounted up to second order products of displacement gradients. For this reason, one may have to quantify the change in surface area up to second order products of surface strains/displacement gradients, and distinguish the surface energy and surface stress measured in the initial surface area or the deformed surface area. Based on this concept the contribution of the surface energy to the system total strain energy will be (Ru 2010, Shaat *et al.* 2013a)

$$\gamma = \tau_0(1 + \varepsilon_{\alpha\alpha}^s) + 0.5(\lambda_0 + \tau_0)(\varepsilon_{\alpha\alpha}^s \varepsilon_{\beta\beta}^s) + (\mu_0 - \tau_0)(\varepsilon_{\alpha\beta}^s \varepsilon_{\alpha\beta}^s) + \tau_0 \Omega \quad ; \alpha, \beta = x, y \quad (6)$$

where γ is the surface strain energy per unit surface area (surface strain energy density), λ_0 and μ_0 are surface Lamé Constants and τ_0 is the pre-surface tension. $\varepsilon_{\alpha\beta}^s$ is the infinitesimal strain tensor at the continuum surface considering the possible deformations (elongation or contraction) induced in the fiber element between two material particles on the surface of the continuum (Eq. (2)). The last term in Eq. (6) depends on all non-zero 3D displacement gradients. Where the sum Ω of 6 squared terms of the second order surface gradient tensor $\nabla_s \mathbf{u}^s = u_{j,\alpha}^s \hat{\mathbf{e}}_\alpha \hat{\mathbf{e}}_j$ (where $\hat{\mathbf{e}}_i$ are unit vectors) is due to the difference between the trace of Lagrangian surface finite strain E^s and the trace of infinitesimal surface strain ε^s (Ru 2010). This clearly explains the cause of the displacement gradient term in Gurtin and Murdoch model and the difference between the Gurtin and Murdoch model and other existing surface elasticity models.

Thus, the constitutive relations of the surface layers as given by Gurtin and Murdoch (1975, 1978) can be extracted from Eq. (6) to be

$$\tau_{\alpha\beta} = \tau_0 \delta_{\alpha\beta} + (\lambda_0 + \tau_0) \varepsilon_{pp}^s \delta_{\alpha\beta} + 2(\mu_0 - \tau_0) \varepsilon_{\alpha\beta}^s + \tau_0 u_{\alpha,\beta}^s \quad (7a)$$

$$\tau_{\alpha k} = \tau_0 u_{k,\alpha}^s \quad (7b)$$

where α, β represent the in-plane Cartesian coordination of the surface, while k represents the out-plane Cartesian coordination of the surface. In Eq. (7), the terms $(\tau_0 u_{\alpha,\beta}^s$ and $\tau_0 u_{k,\alpha}^s)$ are introduced as a consequence of exploiting the Lagrangian surface description and considering the pre-strain developed at the plate surface. In most previous works, theoretical analyses were based on the Eulerian surface elasticity, in which the out-plane terms of surface stress were neglected and the effect of residual stress in the bulk was not taken into account. As an illustration, in this paper, we will consider the effects of these factors on the size-dependent behavior of nano structures.

4. Minimum of total potential energy principle

Based on discussions in previous sections, the total strain energy density is a function of the infinitesimal strain ε_{ij} and the symmetric rotation gradient χ_{ij} of the bulk material, and the infinitesimal strain ε_{ij}^s and the second-order displacement gradient $\nabla^2 \mathbf{u}$ of the surface layer of the structure. This is in the context of the modified couple stress theory in combining with surface elasticity theory.

The potential energy in an elastic plate is the energy contained in the elastic distortions (strain energy) and the capacity of the loads to do work (work done). So, the total potential energy can be written as

$$\Pi = U^B + U^S - J \quad (8)$$

where U^B and U^S are the strain energy of the bulk and the strain energy of the surface of the

continuum, respectively. J is the applied work on the continuum and Π is the total potential energy. From Eq. (4) and Eq. (6), the strain energies U^B and U^S become

$$U^B = \int_V W dV = \frac{1}{2} \int_V (\sigma_{ij} \varepsilon_{ij} + m_{ij} \chi_{ij}) dV \quad (9)$$

$$U^S = \int_A \gamma dA = \frac{1}{2} \int_A (\tau_{\alpha\beta} \varepsilon_{\alpha\beta}^S + \tau_{k\alpha} u_{k,\alpha}^S) dA \quad (10)$$

Thus the equilibrium equation based on the minimization of the total potential energy principle will be

$$\delta U^B + \delta U^S - \delta J = 0 \quad (11)$$

where

$$\delta U^B = \int_V (\sigma_{ij} \delta \varepsilon_{ij} + m_{ij} \delta \chi_{ij}) dV \quad (12)$$

$$\delta U^S = \int_A (\tau_{\alpha\beta} \delta \varepsilon_{\alpha\beta}^S + \tau_{k\alpha} \delta u_{k,\alpha}^S) dA \quad (13)$$

5. Size-dependent elasticity

Here, the size-dependent elasticity model for nano FG Mindlin plates is proposed, incorporating microstructure and surface energy effects, to study the elastic behavior of ultra-thin FG films.

5.1 Displacement and strain fields of Mindlin plate

The Mindlin hypothesis is built up on the assumption that the transverse normals do not remain perpendicular to the mid-plane after deformation. This amounts to include transverse shear strains in the theory. Under the illustrated assumptions, the displacement fields for Mindlin FG plates are of the form

$$\begin{aligned} u_x &= u(x, y, z) = u_0(x, y) + (z + h_0) \phi_x(x, y) \\ u_y &= v(x, y, z) = v_0(x, y) + (z + h_0) \phi_y(x, y) \\ u_z &= \omega(x, y, z) = \omega_0(x, y) \end{aligned} \quad (14)$$

where $(u_0, v_0, \omega_0, \phi_x, \phi_y)$ are unknown functions to be determined and h_0 denotes the position of the neutral plane from the geometrical mid plane (see Fig. 2), where for isotropic homogenous plates $h_0 = 0$. Consequently, from Eq. (2) the nonzero infinitesimal strain components ε_{ij} are given by

$$\begin{aligned} \varepsilon_{xx} &= u_{0,x} + (z + h_0) \phi_{x,x}; \quad \varepsilon_{yy} = v_{0,y} + (z + h_0) \phi_{y,y}; \quad \gamma_{xy} = u_{0,y} + v_{0,x} + (z + h_0) (\phi_{x,y} + \phi_{y,x}) \\ \gamma_{xz} &= \omega_{0,x} + \phi_x; \quad \gamma_{yz} = \omega_{0,y} + \phi_y \end{aligned} \quad (15)$$

Moreover, the components of the rotation vector θ_i and the symmetric part of the rotation gradient tensor χ_{ij} are being associated with the displacement field in Eq. (14), by the following form

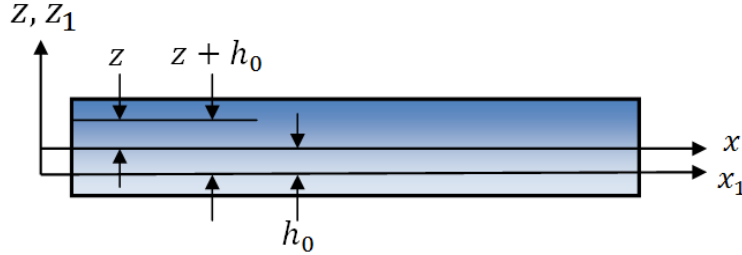


Fig. 2 Coordinate system and geometry of the FG plate.

$$\begin{aligned}\theta_x &= \frac{1}{2}(\omega_{0,y} - \phi_y); \theta_y = \frac{1}{2}(\phi_x - \omega_{0,x}); \\ \theta_z &= \frac{1}{2}((v_{0,x} - u_{0,y}) + (z + h_0)(\phi_{y,x} - \phi_{x,y})) \\ \chi_{xx} &= \frac{1}{2}(\omega_{0,xy} - \phi_{y,x}); \chi_{yy} = \frac{1}{2}(\phi_{x,y} - \omega_{0,xy}); \chi_{zz} = \frac{1}{2}(\phi_{y,x} - \phi_{x,y}); \\ \chi_{xy} &= \frac{1}{4}(\omega_{0,yy} - \omega_{0,xx} + \phi_{x,x} - \phi_{y,y}); \chi_{xz} = \frac{1}{4}[(v_{0,xx} - u_{0,xy}) + (z + h_0)(\phi_{y,xx} - \phi_{x,xy})]; \\ \chi_{yz} &= \frac{1}{4}[(v_{0,xy} - u_{0,yy}) + (z + h_0)(\phi_{y,xy} - \phi_{x,yy})]\end{aligned}\quad (17)$$

5.2 Governing equations

Consider a rectangular FG plate of length a , width b and thickness h subjected to a mechanical transverse load of intensity p . If the surface stresses on the upper and lower surfaces of the plate layers are different and denoted by $\tau_{i\alpha}^+$ and $\tau_{i\alpha}^-$, respectively. By substitution for the virtual strain fields $\delta\varepsilon_{ij}$ and $\delta\chi_{ij}$, with the aid of Eq. (15) and Eq. (17), into Eq. (12) and Eq. (13), the virtual strain energy could be obtained in the form

$$\begin{aligned}\delta U &= \int_A \left\{ - \left(N_{xx,x} + N_{xy,y} + \tau_{xx,x}^+ + \tau_{xx,x}^- + \tau_{xy,y}^+ + \tau_{xy,y}^- + \frac{1}{2}(P_{xz,xy} + P_{yz,yy}) \right) \delta u_0 - \right. \\ &\left(N_{yy,y} + N_{xy,x} + \tau_{yy,y}^+ + \tau_{xy,x}^+ + \tau_{yy,y}^- + \tau_{xy,x}^- - \frac{1}{2}(P_{xz,xx} + P_{yz,xy}) \right) \delta v_0 - \left(N_{xz,x} + N_{yz,y} + \right. \\ &\left. \tau_{xz,x}^+ + \tau_{yz,y}^+ + \tau_{xz,x}^- + \tau_{yz,y}^- + \frac{1}{2}(P_{xy,xx} + P_{yy,xy} - P_{xy,yy} - P_{xx,xy}) \right) \delta \omega_0 - \left(M_{xx,x} + M_{xy,y} - \right. \\ &N_{xz} + \frac{h}{2}(\tau_{xx,x}^+ - \tau_{xx,x}^-) + \frac{h}{2}(\tau_{xy,y}^+ - \tau_{xy,y}^-) + \frac{1}{2}(P_{xy,x} + P_{yy,y} - P_{zz,y} + R_{xz,xy} + R_{yz,yy}) \left. \right) \delta \phi_x - \\ &\left(M_{yy,y} + M_{xy,x} - N_{yz} + \frac{h}{2}(\tau_{yy,y}^+ - \tau_{yy,y}^-) + \frac{h}{2}(\tau_{xy,x}^+ - \tau_{xy,x}^-) - \frac{1}{2}(P_{xy,y} + P_{xx,x} - P_{zz,x} + \right. \\ &\left. R_{xz,xx} + R_{yz,xy}) \right) \delta \phi_y \left. \right\}\end{aligned}\quad (18)$$

where the stress resultants N_{ij} , $M_{\alpha\beta}$, P_{ij} and R_{ij} are defined by

$$N_{ij} = \int_{-h/2}^{h/2} \sigma_{ij} dz \quad (19a)$$

$$M_{\alpha\beta} = \int_{-h/2}^{h/2} (z + h_0) \sigma_{\alpha\beta} dz \quad (19b)$$

$$P_{ij} = \int_{-h/2}^{h/2} m_{ij} dz \quad (19c)$$

$$R_{\alpha z} = \int_{-h/2}^{h/2} (z + h_0) m_{\alpha z} dz \quad (19d)$$

Moreover, the following equivalent stress resultants could be defined

$$N_{\alpha\beta}^* = N_{\alpha\beta} + \tau_{\alpha\beta}^+ + \tau_{\alpha\beta}^- \quad (20a)$$

$$M_{\alpha\beta}^* = M_{\alpha\beta} + \frac{h}{2} (\tau_{\alpha\beta}^+ - \tau_{\alpha\beta}^-) \quad (20b)$$

Consequently, the governing equations in terms of the equivalent resultant forces and moments are given by

$$\begin{aligned} N_{xx,x}^* + N_{xy,y}^* + \frac{1}{2} (P_{xz,xy} + P_{yz,yy}) &= 0 \\ N_{yy,y}^* + N_{xy,x}^* - \frac{1}{2} (P_{xz,xx} + P_{yz,xy}) &= 0 \\ N_{xz,x}^* + N_{yz,y}^* + \frac{1}{2} (P_{xy,xx} + P_{yy,xy} - P_{xy,yy} - P_{xx,xy}) &= p \\ M_{xx,x}^* + M_{xy,y}^* - N_{xz} + \frac{1}{2} (P_{xy,x} + P_{yy,y} - P_{zz,y} + R_{xz,xy} + R_{yz,yy}) &= 0 \\ M_{xy,x}^* + M_{yy,y}^* - N_{yz} - \frac{1}{2} (P_{xy,y} + P_{xx,x} - P_{zz,x} + R_{xz,xx} + R_{yz,xy}) &= 0 \end{aligned} \quad (21)$$

The stress resultants N_{ij}^* , $M_{\alpha\beta}^*$, P_{ij} and $R_{\alpha z}$ for Mindlin FG plate are written explicitly in Appendix A. Then, substitution for the stress resultants N_{ij}^* , $M_{\alpha\beta}^*$, P_{ij} and $R_{\alpha z}$ into Eq. (21) leads to the governing equations in terms of the generalized displacements $(u_0, v_0, \omega_0, \phi_x, \phi_y)$ for FG Mindlin nano plates.

$$\begin{aligned} A_{11}^* u_{0,xx} + A_{12}^* v_{0,xy} + B_{11}^* \phi_{x,xx} + B_{12}^* \phi_{y,xy} + A_{66}^* u_{0,yy} + A_{66}^* v_{0,xy} + B_{66}^* \phi_{x,yy} + B_{66}^* \phi_{y,xy} + \\ \left(\frac{\Delta\tau_0 h v}{2(1-\nu)} + \frac{2\nu h_0 \bar{\tau}_0}{(1-\nu)} \right) \nabla^2(\omega_{0,x}) + \frac{A_n}{4} \nabla^2(v_{0,xy} - u_{0,yy}) + \frac{1}{4} (h_0 A_n + B_n) \nabla^2(\phi_{y,xy} - \phi_{x,yy}) = \\ 0 \end{aligned} \quad (22a)$$

$$\begin{aligned} A_{12}^* u_{0,xy} + A_{22}^* v_{0,yy} + A_{66}^* u_{0,xy} + A_{66}^* v_{0,xx} + B_{66}^* \phi_{x,xy} + B_{66}^* \phi_{y,xx} + B_{12}^* \phi_{x,xy} + B_{22}^* \phi_{y,yy} + \\ \left(\frac{\Delta\tau_0 h v}{2(1-\nu)} + \frac{2\nu h_0 \bar{\tau}_0}{(1-\nu)} \right) \nabla^2(\omega_{0,y}) - \frac{A_n}{4} \nabla^2(v_{0,xx} - u_{0,xy}) - \frac{1}{4} (h_0 A_n + B_n) \nabla^2(\phi_{y,xx} - \phi_{x,xy}) = \\ 0 \end{aligned} \quad (22b)$$

$$\begin{aligned} A_{44}(\omega_{0,xx} + \phi_{x,x}) + 2\bar{\tau}_0 \omega_{0,xx} + A_{55}(\omega_{0,yy} + \phi_{y,y}) + 2\bar{\tau}_0 \omega_{0,yy} - \frac{A_n}{4} \nabla^4 \omega_0 + \frac{A_n}{4} \nabla^2(\phi_{y,y} + \\ \phi_{x,x}) = p \end{aligned} \quad (22c)$$

$$\begin{aligned} B_{11}^{**} u_{0,xx} + B_{12}^{**} v_{0,xy} + B_{66}^{**} u_{0,yy} + B_{66}^{**} v_{0,xy} + D_{11}^* \phi_{x,xx} + D_{12}^* \phi_{y,xy} + D_{66}^* \phi_{x,yy} + D_{66}^* \phi_{y,xy} + \\ A_{44}(\omega_{0,x} + \phi_x) + \left(\frac{\nu(\bar{\tau}_0(h^2 + 12h_0^2) + (3\Delta\tau_0 h h_0))}{6(1-\nu)} \right) \nabla^2(\omega_{0,x}) + \frac{1}{4} (h_0 A_n + B_n) \nabla^2(v_{0,xy} - u_{0,yy}) - \\ \frac{A_n}{4} \nabla^2(\omega_{0,x}) + \frac{A_n}{4} (\phi_{x,xx} + 4\phi_{x,yy} - 3\phi_{y,xy}) + \frac{1}{4} (h_0^2 A_n + 2h_0 B_n + D_n) \nabla^2(\phi_{y,xy} - \phi_{x,yy}) = \\ 0 \end{aligned} \quad (22d)$$

form of governing equations. Also, in Eq. (23) some terms have been added to the classical plate rigidities to incorporate surface effects.

6. Effective mechanical properties of FG plates

In general, many approaches are used for homogenization of FGMs. The choice of the approach should be based on the gradient of gradation relative to the size of a typical representative volume element. In the case where the material properties associated with gradation vary with relatively slow changing functions of spatial coordinates, standard homogenization methods can be applied. Accordingly, the material is assumed locally homogeneous at the representative volume element scale but it is globally heterogeneous on the macroscopic structural scale. However, if the material properties vary rapidly with the coordinates, it is impossible to disregard the heterogeneous nature of the representative volume element. In this case grading is reflected at both microscopic (representative volume element) as well as macroscopic (structural) scales (Shaat *et al.* 2013c).

Many researchers proposed a homogenization models for FGMs, such as the self-consistent models by Hill (1965), the mean field micromechanics models by Mori-Tanaka (1973). Here in this paper the effective Young's Modulus $E(z)$ and the microstructure material length scale $\ell(z)$ of the FG plate will be estimated using the simple Voigt arithmetic method where the distributions of volume fractions through the plate thickness are assumed to follow the simple power law

$$E(z) = E_L + (E_U - E_L) \left(\frac{1}{2} + \frac{z}{h} \right)^n \quad (25a)$$

$$\ell(z) = \ell_L + (\ell_U - \ell_L) \left(\frac{1}{2} + \frac{z}{h} \right)^n \quad (25b)$$

where E_U and ℓ_U , and E_L and ℓ_L are the properties of the upper and lower constituent materials (metal and ceramic), respectively. n can be any non-negative real number and $-\frac{h}{2} \geq z \geq \frac{h}{2}$. The other mechanical properties are expected to have a constant function through the thickness of the plate. The Poisson's ratio for the FG structures may be varying according to a continuous function like Young's modulus. However, in most cases it varies linearly unlike the Young's modulus which will vary according to a nonlinear function (Aboudi 1991). Moreover, based on many previous works (Delale and Erdogan 1983, Chi and Chung 2006), effects of varying the Poisson's ratio have shown fewer contributions to the deformation of FG plates when compared with the Young's modulus. Therefore, assuming a constant Poisson's ratio is acceptable here.

For the analyses of the flexural behavior of a FG plate, subjected only to a transversal applied load, we have to determine the location of the neutral plane before solving the equilibrium equation of the plate. Clearly, due to the varying of Young's modulus of the FG plate through the thickness, the neutral plane is no longer located at the mid-plane but shifted from it. The effect of neutral plane position is typically neglected in most previous studies, while the position of neutral plane for FG plates must be predetermined. To determine the position of the neutral plane, a new coordinate system is constructed such that the new x -axis (x_1 - axis) is placed at the neutral plane (see Fig. 2), (Yaghoobi and Fereidoon 2010, Shaat *et al.* 2013b, c). Moreover, consider an infinitely wide FG plate subjected to a transverse load. The position of the neutral plane can be determined by choosing h_0 such that the axial force at the cross-section vanishes

$$\int_{-\frac{h}{2}}^{\frac{h}{2}} \frac{(z+h_0)E(z)}{1-\nu^2} dz = 0 \tag{26}$$

Consequently, for constant Poisson’s ratio ν through the thickness, the neutral plane is shifted from the mid-plane by

$$h_0 = - \left(\frac{\int_{-\frac{h}{2}}^{\frac{h}{2}} zE(z) dz}{\int_{-\frac{h}{2}}^{\frac{h}{2}} E(z) dz} \right) \tag{27}$$

Eq. (27) provides an applicable way to manage and control the position of neutral plane for FG plates. For design considerations, sometimes we have to adapt the neutral plane position with the required design constraints. Changing the grading continuous function of the FG plate controls the position of the neutral plane (Shaath *et al.* 2013b, c).

7. Analytical solution

In this section, an analytical solution for FG Mindlin simply supported plate is developed. The nano plate is a rectangular plate of length a , width b and thickness h (Fig. 2), and it is subjected to a double Fourier sinusoidal loading

$$p(x, y) = Q \sin \frac{\pi x}{a} \sin \frac{\pi y}{b} \tag{28}$$

The boundary conditions for the simply supported Mindlin plate considering microstructure couple stress and surface energy effects will have the form

$$\begin{cases} v_0 = \omega_0 = \varphi_y = 0 \\ N_{xx}^* + P_{xz,y} = 0 \\ M_{xx}^* + P_{xy} + R_{xz,y} = 0 \end{cases} \quad \text{at } x = 0, a \tag{29a}$$

$$\begin{cases} u_0 = \omega_0 = \varphi_x = 0 \\ N_{yy}^* + P_{yz,x} = 0 \\ M_{yy}^* + P_{xy} + R_{yz,x} = 0 \end{cases} \quad \text{at } y = 0, b \tag{29b}$$

The following displacements expansions will satisfy the boundary condition (Eq. (29)) for the simple supported plate

$$u_o(x, y) = U \sin \alpha \sin \beta \tag{30a}$$

$$v_o(x, y) = V \sin \alpha \sin \beta \tag{30b}$$

$$\omega_o(x, y) = W \sin \alpha \sin \beta \tag{30c}$$

$$\varphi_x(x, y) = X \cos \alpha \sin \beta \tag{30d}$$

$$\varphi_y(x, y) = Y \sin \alpha \cos \beta \tag{30e}$$

where U, V, W, X, Y are coefficients to be determined and $\alpha = \pi x/a$, $\beta = \pi y/b$. We have to mention that, for simply supported plates these classical displacement expansions will satisfy the illustrated boundary conditions. However, for other situations the classical expansions could be adopted to satisfy the inclusion of the surface energy and the microstructure couple stress in the

boundary conditions.

By substituting Eq. (28) and Eq. (30) into Eq. (22), which represent the Mindlin governing equations of nano FG plates, the magnitude coefficients of the degrees of freedom can be obtained by solving the following matrix form

$$\begin{bmatrix} s_{11}^* & s_{12}^* & s_{13}^* & s_{14}^* & s_{15}^* \\ s_{21}^* & s_{22}^* & s_{23}^* & s_{24}^* & s_{25}^* \\ 0 & 0 & s_{33}^* & s_{34}^* & s_{35}^* \\ s_{41}^* & s_{42}^* & s_{43}^* & s_{44}^* & s_{45}^* \\ s_{51}^* & s_{52}^* & s_{53}^* & s_{54}^* & s_{55}^* \end{bmatrix} \begin{Bmatrix} U \\ V \\ W \\ X \\ Y \end{Bmatrix} = \begin{Bmatrix} 0 \\ 0 \\ Q \\ 0 \\ 0 \end{Bmatrix} \quad (31)$$

where s_{ij}^* are

$$\begin{aligned} s_{11}^* &= \alpha^2 A_{11}^* + \beta^2 A_{66}^* + \frac{A_n}{4} \beta^2 (\alpha^2 + \beta^2); \\ s_{12}^* &= s_{21}^* = \alpha \beta (A_{12}^* + A_{66}^*) - \frac{A_n}{4} \alpha \beta (\alpha^2 + \beta^2); \\ s_{13}^* &= (\alpha^3 + \beta^2 \alpha) \left(\frac{\Delta \tau_0 h v}{2(1-v)} + \frac{2v h_0 \bar{\tau}_0}{(1-v)} \right); \\ s_{14}^* &= \alpha^2 B_{11}^* + \beta^2 B_{66}^* + \frac{1}{4} (h_0 A_n + B_n) \beta^2 (\alpha^2 + \beta^2); \\ s_{15}^* &= \alpha \beta (B_{12}^* + B_{66}^*) - \frac{1}{4} (h_0 A_n + B_n) \alpha \beta (\alpha^2 + \beta^2); \\ s_{22}^* &= \alpha^2 A_{66}^* + \beta^2 A_{22}^* + \frac{A_n}{4} \alpha^2 (\alpha^2 + \beta^2); \\ s_{23}^* &= (\beta^3 + \alpha^2 \beta) \left(\frac{\Delta \tau_0 h v}{2(1-v)} + \frac{2v h_0 \bar{\tau}_0}{(1-v)} \right); \\ s_{24}^* &= \alpha \beta (B_{12}^* + B_{66}^*) - \frac{1}{4} (h_0 A_n + B_n) \alpha \beta (\alpha^2 + \beta^2); \\ s_{25}^* &= \alpha^2 B_{66}^* + \beta^2 B_{22}^* + \frac{1}{4} (h_0 A_n + B_n) \alpha^2 (\alpha^2 + \beta^2); \\ s_{33}^* &= \alpha^2 (A_{44} + 2\bar{\tau}_0) + \beta^2 (A_{55} + 2\bar{\tau}_0) + \frac{A_n}{4} (\alpha^2 + \beta^2)^2; \\ s_{34}^* &= \alpha A_{44} - \frac{A_n}{4} \alpha (\alpha^2 + \beta^2); \\ s_{35}^* &= \beta A_{55} - \frac{A_n}{4} \beta (\alpha^2 + \beta^2); \\ s_{41}^* &= \alpha^2 B_{11}^{**} + \beta^2 B_{66}^{**} + \frac{1}{4} (h_0 A_n + B_n) \beta^2 (\alpha^2 + \beta^2); \\ s_{42}^* &= \alpha \beta (B_{12}^{**} + B_{66}^{**}) - \frac{1}{4} (h_0 A_n + B_n) \alpha \beta (\alpha^2 + \beta^2); \\ s_{43}^* &= \alpha A_{44} + \left(\left(\frac{v (\bar{\tau}_0 (h^2 + 12h_0^2) + (3\Delta \tau_0 h h_0))}{6(1-v)} \right) (\alpha^3 + \beta^2 \alpha) \right) - \frac{A_n}{4} \alpha (\alpha^2 + \beta^2); \\ s_{44}^* &= \alpha^2 D_{11}^* + \beta^2 D_{66}^* + A_{44} + \frac{1}{4} (h_0^2 A_n + 2h_0 B_n + D_n) \beta^2 (\alpha^2 + \beta^2) + \frac{A_n}{4} (\alpha^2 + 4\beta^2); \end{aligned}$$

$$\begin{aligned}
 s_{45}^* = s_{54}^* &= \alpha\beta(D_{12}^* + D_{66}^*) - \frac{1}{4}(h_0^2 A_n + 2h_0 B_n + D_n)\alpha\beta(\alpha^2 + \beta^2) - \frac{3A_n}{4}\alpha\beta \\
 s_{51}^* &= \alpha\beta(B_{12}^{**} + B_{66}^{**}) - \frac{1}{4}(h_0 A_n + B_n)\alpha\beta(\alpha^2 + \beta^2); \\
 s_{52}^* &= \alpha^2 B_{66}^{**} + \beta^2 B_{22}^{**} + \frac{1}{4}(h_0 A_n + B_n)\alpha^2(\alpha^2 + \beta^2); \\
 s_{53}^* &= \beta A_{55} + \left(\left(\frac{v(\bar{\tau}_0(h^2 + 12h_0^2) + (3\Delta\tau_0 h h_0))}{6(1-v)} \right) (\alpha^2\beta + \beta^3) \right) - \frac{A_n}{4}\beta(\alpha^2 + \beta^2); \\
 s_{55}^* &= \alpha^2 D_{66}^* + \beta^2 D_{22}^* + A_{55} + \frac{1}{4}(h_0^2 A_n + 2h_0 B_n + D_n)\alpha^2(\alpha^2 + \beta^2) + \frac{A_n}{4}(\beta^2 + 4\alpha^2) \quad (32)
 \end{aligned}$$

8. Numerical results

In this section, some numerical examples are performed for a simply supported FG plate to verify the present model and to provide a suitable parametric study. The plate has a length a , a width b and a thickness h and it is expected to be functionally graded according to the simple power law of a two constituent materials (Al and Si) through its thickness. Moreover, it is subjected to a sinusoidal distributed mechanical load of intensity p . Throughout this section, effects of surface energy, microstructure couple stress, grading parameter n considering the exact neutral plane position on the bending behavior of FG ultra-thin films are studied.

8.1 Model verification

In this subsection, the case studies solved by Thai and Choi (2013), Shaat *et al.* (2013b) are reconsidered here to verify the proposed present model for the inclusion of the couple stress effects and the inclusion of surface effects, respectively.

Thai and Choi (2013) studied the effect of the length scale parameter ℓ and the grading parameter n on the static deflection of a square simply supported FG plate whose material and geometrical parameters are: $E_U=14.4$ GPa; $E_L=1.44$ GPa; $\nu_U=\nu_L=0.38$; $h=17.6$ μm ; $p=1$ Pa. In this study, Thai and Choi assumed a constant material length scale parameter ℓ through the plate thickness. Table 1 shows a comparison between the nondimensional maximum deflection ($\bar{\omega} = (100E_L h^3 / p a^4) \times \omega(a/2, b/2)$) predicted by Thai and Choi model and predicted by the present model. The table shows a high agreement between the results of the present model and those of Thai and Choi (2013) model.

Now, consider an Al/Si infinitely wide isotropic FG plate with $a/h = 10$ to study the effect of grading parameter n in combining with surface energy effects on its bending behavior. This case study is previously considered by Shaat *et al.* (2013b) thus the plate is subjected to a sinusoidal load of intensity $p = 1$ Pa and has the following material parameters: $E_U = 210$ GPa; $E_L = 68.5$ GPa; $\nu_U = \nu_L = 0.35$. Fig. 3 shows the non-dimensional difference between the central deflection predicted by the surface elasticity model (neglecting couple stress effects) and the classical elasticity model $((\omega^S - \omega^C) / \omega^C)$ for different values of the grading parameter n . The figure reflects the great effect of the plate surface energy and surface tension on its deflection. Moreover the figured results shows a great agreement with those presented in Shaat *et al.* (2013b).

Table 1 Non-dimensional central deflection $\bar{\omega} = (100E_L h^3 / \rho a^4) \times \omega(a/2, b/2)$ of a simply supported square plate ($h = 17.6 \mu m$) (neglecting surface energy effects)

a/h	ℓ_U/h	$n = 0$		$n = 1$		$n = 10$	
		Thai and Choi (2013)	Present Model	Thai and Choi (2013)	Present Model	Thai and Choi (2013)	Present Model
5	0	0.3306	0.3306	0.7387	0.73875	1.6898	1.6898
	0.2	0.2876	0.2876	0.6200	0.6199	1.4867	1.4867
	0.4	0.2086	0.20856	0.4224	0.4224	1.1010	1.1010
	0.6	0.1456	0.14564	0.2817	0.2817	0.7818	0.78176
	0.8	0.1049	0.10491	0.1974	0.19738	0.5691	0.5691
	1	0.0793	0.0793	0.1469	0.14685	0.4328	0.4328
10	0	0.2803	0.2803	0.6472	0.6472	1.4130	1.41299
	0.2	0.2440	0.24402	0.5433	0.5433	1.2444	1.2444
	0.4	0.1762	0.1762	0.3678	0.3678	0.9186	0.9186
	0.6	0.1211	0.1211	0.2406	0.24056	0.6429	0.64288
	0.8	0.0849	0.08491	0.1635	0.16346	0.4561	0.45614
	1	0.0619	0.0619	0.1169	0.1169	0.3352	0.3352
20	0	0.2677	0.2677	0.6243	0.62434	1.3438	1.3438
	0.2	0.2330	0.2330	0.5240	0.52403	1.1834	1.18339
	0.4	0.1680	0.16796	0.3539	0.35385	0.8719	0.8719
	0.6	0.1148	0.11478	0.2300	0.2299	0.6069	0.6069
	0.8	0.0797	0.0797	0.1547	0.15468	0.4266	0.4266
	1	0.0574	0.05736	0.1092	0.10916	0.3095	0.3095

8.2 Parametric study

In this subsection, effects of the microstructure couple stress and surface energy on the bending behavior of FG simply supported plates are investigated. To this aim, consider a simply supported rectangular FG plate with the material parameters shown in Table 2.

Fig. 4 shows the non-dimensional difference between central deflection predicted by the modified couple stress model (neglecting surface effects) and the classical elasticity model $((\omega^M - \omega^C)/\omega^C)$ for different grading parameter n for range of plate thickness ($h = 1 \mu m \rightarrow 50 \mu m$). The results show that the FG and the homogenous plates provide negative non-dimensional differences, which means that the length scale parameter $\ell(z)$ stiffens the plate. Moreover, the effect of the couple stress appears in micro scale thicknesses for FG plates and Al plate, while the Si plate provides a negligible sense with the couple stress effects for this range of plate thickness. This action depends basically on the value of the material parameter ℓ for both Al and Si materials. The figure shows, also, a decrease in the non-dimensional difference by increasing the grading parameter n , this is for FG plate whose upper material parameter ℓ_U is smaller than its lower material parameter ℓ_L .

Fig. 5 represents the surface energy effects on the behavior of FG and homogenous plates. The figure shows the non-dimensional difference between central deflection predicted by the surface elasticity model (neglecting couple stress effects) and the classical elasticity model $((\omega^S - \omega^C)/\omega^C)$ for different grading parameter n for range of plate thickness ($h = 1 nm \rightarrow 50 nm$). For this

case of FG plate, the plate surface tension in addition to the surface Lamé constants stiffens the plate. We have to mention that, surface energy and surface tension could stiffen or soften the plate depending on the plate surface properties. While the microstructure couple stress always adds additional stiffness to the plate.

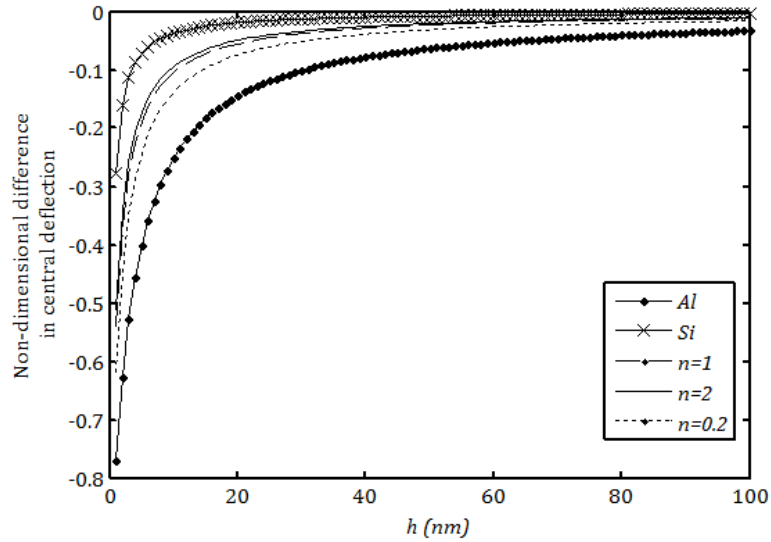


Fig. 3 Non-dimensional difference in central deflection $(\omega^S - \omega^C)/\omega^C$ versus plate thickness for different grading parameter n (neglecting couple stress effects).

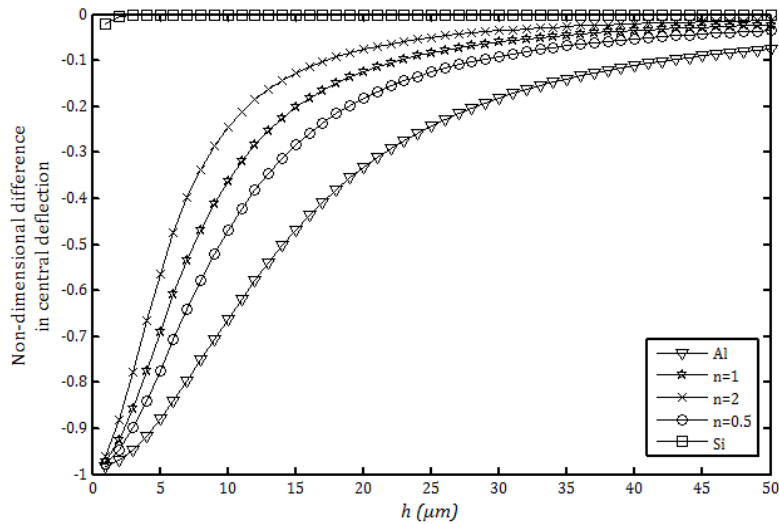


Fig. 4 Non-dimensional difference in central deflection $(\omega^M - \omega^C)/\omega^C$ versus plate thickness for different grading parameter n . ($a = b = 10h$; $\bar{P} = 2^*$) (Neglecting surface energy effects)*
Dimensionless load parameter $\bar{P} = \frac{pa^4}{E_U h^4}$.

Table 2 Material Properties of the FG plate (Shaat *et al.* 2013b, c, Rokni *et al.* 2013, Gao and Mahmoud 2014, Shaat and Mohamed 2014)

Property	Aluminum (Upper surface)	Silicon (upper surface)
Young's modulus	$E_U = 90 \text{ GPa}$	$E_L = 210 \text{ GPa}$
Poisson's ratio	$\nu_U = 0.23$	$\nu_L = 0.23$
Surface tension	$\tau_{0U} = 0.5689 \text{ N/m}$	$\tau_{0L} = 0.605 \text{ N/m}$
Surface Lama constants	$\mu_{0U} = -5.4251, \lambda_{0L} = 3.4939 \text{ N/m}$	$\mu_{0L} = -2.774, \lambda_{0U} = -4.488 \text{ N/m}$
Microstructure parameter	$\ell_U = 6.58 \mu\text{m}$	$\ell_L = 65 \text{ nm}$

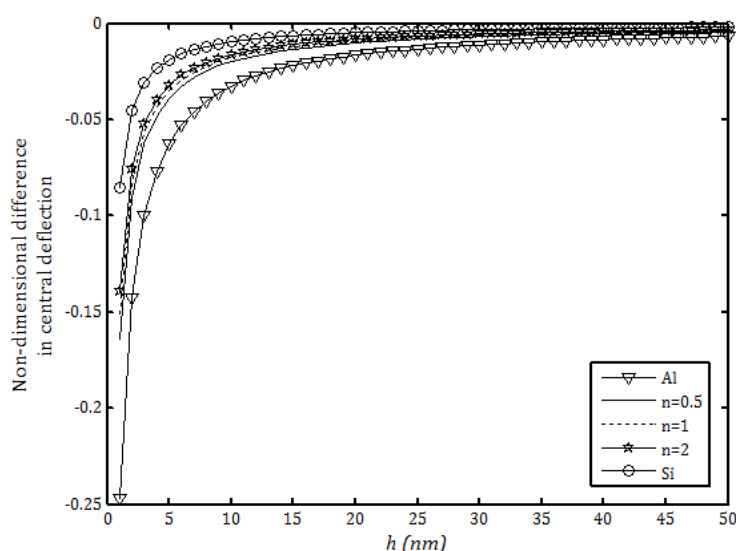
Fig. 5 Non-dimensional difference in central deflection $(\omega^S - \omega^C)/\omega^C$ versus plate thickness for different grading parameter n . ($a = b = 10h$; $\bar{P} = 2$) (Neglecting couple stress effects).

Fig. 6 represents the non-dimensional central deflection (ω/h) distribution along the plate length for different ℓ_U/h ratios and for different ℓ_L/ℓ_U ratios. The figure reflects the great effect of the couple stress on the plate deflection which records the highest effects at $\ell_U/h = 1$ and $\ell_L/\ell_U = 1$. Moreover, increasing ℓ_L/ℓ_U ratio reduces the plate deflection. By comparing the results of Fig. 6(a) and Fig. 6(b), the surface tension will stiffen the plate and hence reduces the plate deflection. This figure reflects the great effect of both of surface energy and couple stress on the bending behavior of the FG plate.

Based on the proposed model, comprehensive results of non-dimensional deflection are also tabulated in Table 3 and Table 4 for various cases of including or not including the couple stress effect and surface energy effect for homogenous ($n = 0$) and FG ($n \neq 0$) plates. These results can be used for evaluating the reliability of size-dependent plate models developed in the future. The table shows a decrease in the plate non-dimensional central deflection ($\bar{\omega} = 100E_U h^3 \omega / p a^4$) by increasing the grading parameter n (this is for a FG plate with $E_U/E_L < 1$). Observing the numerical values in the table shows that the difference in deflection when considering and neglecting the surface effects reduces by increasing the grading parameter n . Moreover,

Table 3 Non-dimensional central deflection \bar{w} of a simply supported square plate ($h = 1 \mu\text{m}$)

a/h	ℓ_L/ℓ_U	ℓ_U/h	$n = 0$		$n = 1$		$n = 2$	
			WSE ¹	NSE ²	WSE	NSE	WSE	NSE
5	0.01	0	3.5158	3.5151	2.2079	2.2076	2.0113	2.0110
		0.2	2.9669	2.9664	2.0968	2.0965	1.9520	1.9518
		0.4	2.0404	2.0402	1.8236	1.8234	1.7942	1.7940
		0.6	1.3695	1.3694	1.5028	1.5027	1.5829	1.5827
		0.8	0.9632	0.9632	1.2118	1.2117	1.3615	1.3614
		1	0.7181	0.7181	0.9765	0.9765	1.1573	1.1572
	0.1	0	3.5158	3.5151	2.2079	2.2076	2.0113	2.0110
		0.2	2.9669	2.9664	2.0836	2.0833	1.9411	1.9409
		0.4	2.0404	2.0402	1.7849	1.7847	1.7582	1.7580
		0.6	1.3695	1.3694	1.4460	1.4459	1.5218	1.5217
		0.8	0.9632	0.9632	1.1490	1.1490	1.2842	1.2841
		1	0.7181	0.7181	0.9160	0.9159	1.0734	1.0733
	1	0	3.5158	3.5151	2.2079	2.2076	2.0113	2.0110
		0.2	2.9669	2.9664	1.8473	1.8471	1.6723	1.6722
		0.4	2.0404	2.0402	1.2524	1.2524	1.1224	1.1224
		0.6	1.3695	1.3694	0.8322	0.8322	0.7407	0.7407
		0.8	0.9632	0.9632	0.5820	0.5820	0.5159	0.5159
		1	0.7181	0.7181	0.4325	0.4325	0.3826	0.3826
20	0.01	0	2.9468	2.9543	1.8682	1.8712	1.7116	1.7141
		0.2	2.4884	2.4937	1.7748	1.7775	1.6616	1.6639
		0.4	1.6978	1.7003	1.5434	1.5455	1.5276	1.5296
		0.6	1.1118	1.1129	1.2683	1.2696	1.3468	1.3483
		0.8	0.7513	0.7518	1.0153	1.0162	1.1555	1.1566
		1	0.5317	0.5320	0.8085	0.8091	0.9773	0.9781
	0.1	0	2.9468	2.9543	1.8682	1.8712	1.7116	1.7141
		0.2	2.4884	2.4937	1.7637	1.7663	1.6523	1.6547
		0.4	1.6978	1.7003	1.5104	1.5124	1.4969	1.4988
		0.6	1.1118	1.1129	1.2191	1.2204	1.2942	1.2957
		0.8	0.7513	0.7518	0.9603	0.9611	1.0882	1.0892
		1	0.5317	0.5320	0.7549	0.7554	0.9035	0.9042
	1	0	2.9468	2.9543	1.8682	1.8712	1.7116	1.7141
		0.2	2.4884	2.4937	1.5636	1.5657	1.4235	1.4253
		0.4	1.6978	1.7003	1.0508	1.0518	0.9467	0.9475
		0.6	1.1118	1.1129	0.6806	0.6810	0.6085	0.6088
		0.8	0.7513	0.7518	0.4568	0.4570	0.4066	0.4067
		1	0.5317	0.5320	0.3220	0.3221	0.2858	0.2859

¹WSE: With surface energy (considering surface energy effects)

²NSE: Without surface energy (Neglecting surface energy effects)

considering the couple stress effect reduces the contribution of the surface energy on the plate deflection which records the minimum values at $\ell_U/h = 1$. Also, the table reflects the great effect of the couple stress on the plate deflection which records the highest effect at $\ell_U/h = 1$. Moreover, it is observed that the microstructure effects on deflection, through the application of the modified-couple stress theory, is higher than that caused by the surface energy effect for $\ell_U/h = 1$.

Table 4 Non-dimensional central deflection \bar{w} of a simply supported square plate ($h = 1 \text{ nm}$)

a/h	ℓ_L/ℓ_U	ℓ_U/h	$n = 0$		$n = 1$		$n = 2$	
			WSE	NSE	WSE	NSE	WSE	NSE
5	0.01	0	4.7659	3.5151	2.6025	2.2076	2.3396	2.0110
		0.2	3.7415	2.9664	2.4419	2.0965	2.2563	1.9518
		0.4	2.3049	2.0402	2.0634	1.8234	2.0394	1.7940
		0.6	1.4416	1.3694	1.6457	1.5027	1.7601	1.5827
		0.8	0.9763	0.9632	1.2898	1.2117	1.4805	1.3614
		1	0.7138	0.7181	1.0167	0.9765	1.2334	1.1572
	0.1	0	4.7659	3.5151	2.6025	2.2076	2.3396	2.0110
		0.2	3.7415	2.9664	2.4232	2.0833	2.2411	1.9409
		0.4	2.3049	2.0402	2.0115	1.7847	1.9909	1.7580
		0.6	1.4416	1.3694	1.5745	1.4459	1.6817	1.5217
		0.8	0.9763	0.9632	1.2157	1.1490	1.3857	1.2841
		1	0.7138	0.7181	0.9484	0.9159	1.1347	1.0733
	1	0	4.7659	3.5151	2.6025	2.2076	2.3396	2.0110
		0.2	3.7415	2.9664	2.0953	1.8471	1.8768	1.6722
		0.4	2.3049	2.0402	1.3382	1.2524	1.1922	1.2240
		0.6	1.4416	1.3694	0.8553	0.8322	0.7594	0.7407
		0.8	0.9763	0.9632	0.5857	0.5820	0.5190	0.5159
		1	0.7138	0.7181	0.4305	0.4325	0.3811	0.3826
20	0.01	0	0.8415	2.9543	0.7202	1.8712	0.6959	1.7141
		0.2	0.7992	2.4937	0.7058	1.7775	0.6875	1.6639
		0.4	0.6946	1.7003	0.6660	1.5455	0.6633	1.5296
		0.6	0.5707	1.1129	0.6088	1.2696	0.6267	1.3483
		0.8	0.4573	0.7518	0.5435	1.0162	0.5817	1.1566
		1	0.3650	0.5320	0.4778	0.8091	0.5326	0.9781
	0.1	0	0.8415	2.9543	0.7202	1.8712	0.6959	1.7141
		0.2	0.7992	2.4937	0.7041	1.7663	0.6859	1.6547
		0.4	0.6946	1.7003	0.6597	1.5124	0.6575	1.4988
		0.6	0.5707	1.1129	0.5972	1.2204	0.6150	1.2957
		0.8	0.4573	0.7518	0.5273	0.9611	0.5641	1.0892
		1	0.3650	0.5320	0.4585	0.7554	0.5099	0.9042
	1	0	0.8415	2.9543	0.7202	1.8712	0.6959	1.7141
		0.2	0.7992	2.4937	0.6697	1.5657	0.6429	1.4253
		0.4	0.6946	1.7003	0.5536	1.0518	0.5234	0.9475
		0.6	0.5707	1.1129	0.4299	0.6810	0.4001	0.6088
		0.8	0.4573	0.7518	0.3280	0.4570	0.3013	0.4067
		1	0.3650	0.5320	0.2519	0.3221	0.2293	0.2859

Moreover, increasing the a/h ratio increases the contribution of the surface energy on the plate deflection. On the other hand, the couple stress effects reduce by increasing the a/h ratio. For lower a/h ratios, the trend of the surface energy is to soften the plate, while, for higher ratios, the surface energy will stiffen the plate. This reflects the great effect of the transverse shear strain, which included in the Mindlin plate theory, in combining with the surface energy on the bending behavior of FG ultra-thin plates (Shaat *et al.* 2013b, c).

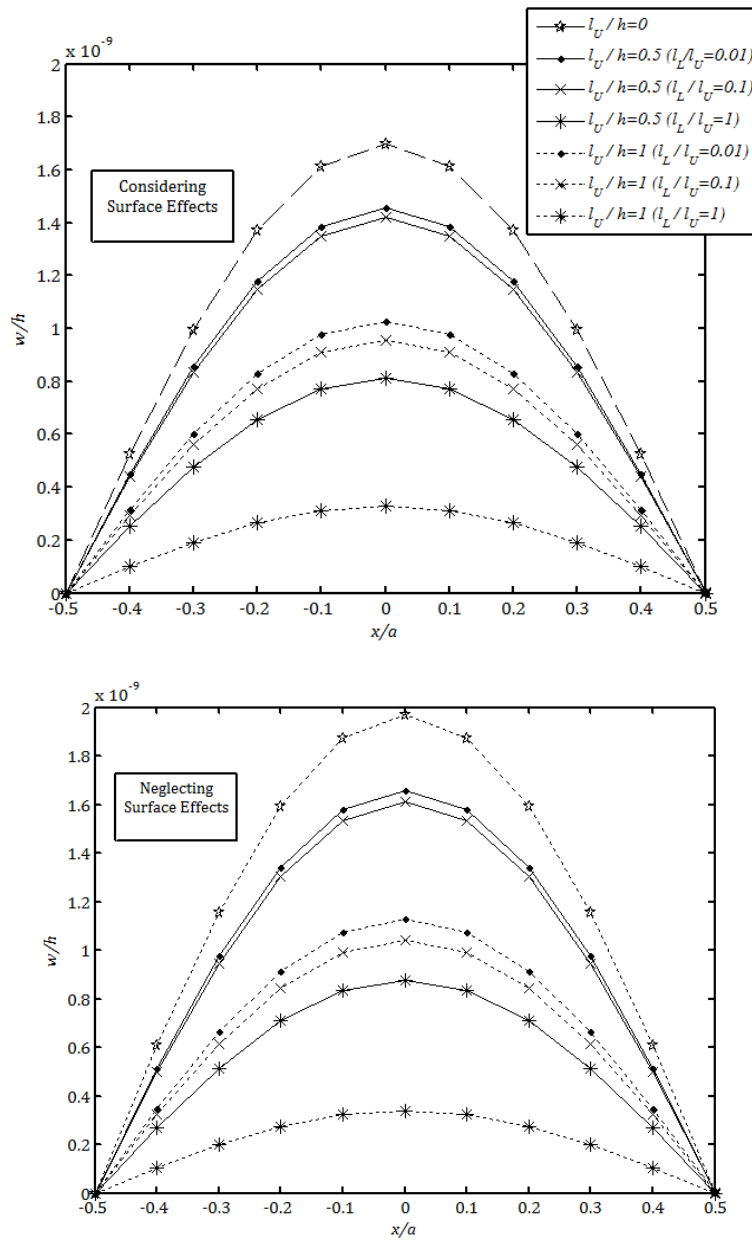


Fig. 6 Non-dimensional central deflection distribution along the plate length for different ℓ_U/h and ℓ_U/ℓ_L ratios. ($a = b = 10h$; $p = 1 Pa$; $n = 2$).

Also when considering couple stress effects and neglecting surface energy effects, the table records the same values for both of $h = 1\mu m$ and $h = 1 nm$. Moreover, for micro-scale thickness the effect of surface energy is negligible and increases as reducing the plate thickness to nano scale thickness.

9. Conclusions

Here, the essential kinematical and kinetical relations for nano continuum mechanics of nano solids are derived and discussed. The fundamental equations and relations for the modified couple stress theory are derived to illustrate the microstructure effects on micro/nano solids. Moreover, the effect of the material surface free energy is incorporated into the modified continuum theory. Through the paper, the governing equations for the size-dependent model for Mindlin nano FG plates are derived and analytically solved to provide a parametric study. As a consequence, some conclusions are extracted:

- Each of the plate surface energy and microstructure couple stress has a significant effect on its bending behavior which will be more significant when working together.
- For very small plate thicknesses, the microstructure couple stress will be significant and records the highest contributions for $\ell/h = 1$.
- Comparing to the effect of microstructure couple stress, the effect of surface energy reduces by increasing ℓ/h ratio.
- There is a great effect of the transverse shear strain in combining with the surface energy on the bending behavior of FG ultra-thin plates.
- Increasing a/h ratio increases the contributions of surface energy and reduces the contribution of the microstructure couple stress.
- The classical continuum theories provide a misleading estimation of the behavior of nanosolids. Consequently, the classical theories are adopted to provide an acceptable estimation for the unique behavior of nanosolids that is relevant to experimental estimations.

References

- Aboudi, J. (1991), *Mechanics of Composite Materials - A Unified Micromechanical Approach*, Elsevier, Amsterdam.
- Alibeigloo, A. (2010), "Exact solution for thermo-elastic response of functionally graded rectangular plates", *Compos. Struct.*, **92**, 113-121.
- Alieldin, S.S., Alshorbagy, A.E. and Shaat, M. (2011), "A first-order shear deformation finite element model for elastostatic analysis of laminated composite plates and the equivalent functionally graded plates", *Ain Sham. Eng. J.*, **2**, 53-6.
- Alshorbagy, A.E., Alieldin, S.S., Shaat, M. and Mahmoud, F.F. (2013), "Finite element analysis of the deformation of functionally graded plates under thermomechanical loads", *Math. Prob. Eng.*, **2013**, 13.
- Arbind, A. and Reddy, J.N. (2013), "Nonlinear analysis of functionally graded microstructure-dependent beams", *Compos. Struct.*, **98**, 272-281.
- Bafekrpour, E., Simon, G.P., Habsuda, J., Naebe, M., Yang, C. and Fox, B. (2012), "Fabrication and characterization of functionally graded synthetic graphite/phenolic nanocomposites", *Mater. Sci. Eng. A*, **545**, 123-131.
- Bharti, I., Gupta, N. and Gupta, K.M. (2013), "Novel applications of functionally graded nano, optoelectronic and thermoelectric materials", *Int. J. Mater. Mech. Manuf.*, **1**(3), 221-224.
- Birman, V. and Byrd, L.W. (2007), "Modeling and analysis of functionally graded materials and structures", *Appl. Mech. Rev.*, **60**, 195-216.
- Chen, Y., Lee, J.D. and Eskandarian, A. (2004), "Atomistic viewpoint of the applicability of micro continuum theories", *Int. J. Solid. Struct.*, **41**, 2085-2097.
- Chi, S.H. and Chung, Y.L. (2006), "Mechanical behavior of functionally graded material plates under transverse load-Part I: analysis", *Int. J. Solid. Struct.*, **43**, 3657-3674.

- Chong, A.C.M., Yang, F., Lam, D.C.C. and Tong, P. (2001), "Torsion and bending of micron-scaled structures", *J. Mater. Res.*, **16**(4), 1052-8.
- Cosserat, E. and Cosserat, F. (1909), *Theory of deformable bodies*, A. Hermann etFils, Paris.
- Delale, F. and Erdogan, F. (1983), "The crack problem for a nonhomogeneous plane", *ASME J. Appl. Mech.*, **50**, 609-614.
- Edelen, D.G.B. (1969), "Protoelastic bodies with large deformation", *Arch. Rat. Mech. Anal.*, **34**, 283-300.
- Eringen, A.C. and Suhubi, E.S. (1964), "Nonlinear theory of simple micro-elastic solids-I", *Int. J. Eng. Sci.*, **2**, 189-203.
- Eringen, A.C. (1966), "A unified theory of thermomechanical materials", *Int. J. Eng. Sci.*, **4**, 179-202.
- Eringen, A.C. (1999), *Microcontinuum Field Theories I: Foundations and Solids*, Springer-Verlag, New York.
- Fu, Y. and Zhang, J. (2010), "Modeling and analysis of microtubules based on a modified couple stress theory", *Phys. E: Low-Dimen. Syst. Nanostruct.*, **42**(5), 1741-5.
- Gao, X.L. and Mahmoud, F.F. (2014), "A new Bernoulli-Euler beam model incorporating microstructure and surface energy effects", *Z. Angew. Math. Phys.*, **65** (2), 393-404.
- Guo, J.G. and Zhao, Y.P. (2005), "The size-dependent elastic properties of nanofilms with surface effects", *J. Appl. Phys.*, **98**, 11.
- Guo, J.G. and Zhao, Y.P. (2007), "The size-dependent bending elastic properties of nanobeams with surface effects", *Nanotechnol.*, **18**, 6.
- Gurtin, M.E. and Murdoch, A.I. (1975), "A continuum theory of elastic material surface", *Arch. Ration. Mech. Anal.*, **57**, 291-323.
- Gurtin, M.E. and Murdoch, A.I. (1978), "Surface stress in solids", *Int. J. Solid. Struct.*, **14**, 431-440.
- Hadjefandiari, A.R. and Dargush, G.F. (2011), "Couple stress theory for solids", *Int. J. Solid. Struct.*, **48**, 2496-2510.
- Hill, R. (1965), "A self-consistent mechanics of composite materials", *J. Mech. Phys. Solid.*, **13**, 213-222.
- Jomehzadeh, E., Noori, H.R. and Saidi, A.R. (2011), "The size-dependent vibration analysis of micro plates based on a modified couple stress theory", *Phys. E: Low-Dimen. Syst. Nanostruct.*, **43**(4), 877-83.
- Kahrobaiyan, M.H., Asghari, M., Rahaeifard, M. and Ahmadian, M.T. (2010), "Investigation of the size-dependent dynamic characteristics of atomic force microscope microcantilevers based on the modified couple stress theory", *Int. J. Eng. Sci.*, **48**(12), 1985-94.
- Ke, L.L. and Wang, Y.S. (2011), "Flow-induced vibration and instability of embedded doublewalled carbon nanotubes based on a modified couple stress theory", *Phys. E: Low-Dimens. Syst. Nanostruct.*, **43**(5), 1031-9.
- Ke, L.L., Wang, Y.S. and Wang, Z.D. (2011), "Thermal effect on free vibration and buckling of size-dependent microbeams", *Phys. E: Low-Dimens. Syst. Nanostruct.*, **43**(7), 1387-93.
- Ke, L.L., Wang, Y.S., Yang, J. and Kitipornchai, S. (2012), "Free vibration of size-dependent Mindlinmicroplates based on the modified couple stress theory", *J. Sound. Vib.*, **331**(1), 94-106.
- Koiter, W.T. (1964), "Couple stresses in the theory of elasticity, I and II", *Nederl. Akad. Wetensch. Proc. Ser. B*, **67**, 17-44.
- Kong, S., Zhou, S., Nie, Z. and Wang, K. (2008), "The size-dependent natural frequency of Bernoulli-Euler micro-beams", *Int. J. Eng. Sci.*, **46**(5), 427-37.
- Lam, D.C.C., Yang, F., Chong, A.C.M., Wang, J. and Tong, P. (2003), "Experiments and theory in strain gradient elasticity", *J. Mech. Phys. Solid.*, **51**(8), 1477-508.
- Lu, P., He, L.H. and Lu, C. (2006), "Thin plate theory including surface effects", *Int. J. Solid. Struct.*, **43** (16), 4631-4647.
- Lü, C.F., Lim, C.W. and Chen, W.Q. (2009), "Size-dependent elastic behavior of FGM ultra-thin films based on generalized refined theory", *Int. J. Solid. Struct.*, **46**, 1176-1185.
- Ma, H.M., Gao, X.L. and Reddy, J.N. (2008), "A microstructure-dependent Timoshenko beam model based on a modified couple stress theory", *J. Mech. Phys. Solids*, **56**(12), 3379-91.
- Ma, H.M., Gao, X.L. and Reddy, J.N. (2011), "A non-classical Mindlin plate model based on a modified

- couple stress theory”, *Acta. Mech.*, **220**(1-4), 217-35.
- Mahmoud, F.F., Eltahir, M.A., Alshorbagy, A.E. and Meletis, E.I. (2012), “Static analysis of nanobeams including surface effects by nonlocal finite element”, *J. Mech. Sci. Technol.*, **26**(11), 3555-3563.
- Mindlin, R.D. and Tiersten, H.F. (1962), “Effects of couple stresses in linear elasticity”, *Arch. Rational Mech. Anal.*, **11**, 415-448.
- Mindlin, R.D. (1964), “Microstructure in linear elasticity”, *Arch. Rational Mech. Anal.*, **16**, 51-78.
- Mori, T. and Tanaka, K. (1973), “Average stress in matrix and average elastic energy of materials with misfitting inclusions”, *Acta. Metall.*, **21**, 571-574.
- Park, S.K. and Gao, X.L. (2006), “Bernoulli–Euler beam model based on a modified couple stress theory”, *J. Micromech. Microeng.*, **16**, 2355.
- Rokni, H., Seethaler, R.J., Milani, A.S., Hashemi, S.H. and Li, X.F. (2013), “Analytical closed-form solutions for size-dependent static pull-in behavior in electrostatic micro-actuators via Fredholm integral equation”, *Sens. Actuat. A*, **190**, 32-43.
- Ru, C.Q. (2010), “Simple geometrical explanation of Gurtin-Murdoch model of surface elasticity with clarification of its related versions”, *J. Phys. Mech. Astron.*, **53**, 536-544.
- Shaat, M., Mahmoud, F.F., Alshorbagy, A.E., Alieldin, S.S. and Meletis, E.I. (2012), “Size-dependent analysis of functionally graded ultra-thin films”, *Struct. Eng. Mech.*, **44**(4), 431-448.
- Shaat, M., Eltahir, M.A., Gad, A.I. and Mahmoud, F.F. (2013a), “Nonlinear size-dependent finite element analysis of functionally graded elastic tiny-bodies”, *Int. J. Mech. Sci.*, **77**, 356-64.
- Shaat, M., Mahmoud, F.F., Alshorbagy, A. E. and Alieldin, S. S. (2013b), “Bending Analysis of Ultra-thin Functionally Graded Mindlin Plates Incorporating Surface Energy Effects”, *International Journal of Mechanical Sciences*, **75**, 223-232.
- Shaat, M., Mahmoud, F.F., Alieldin, S.S. and Alshorbagy, A.E. (2013c), “Finite element analysis of functionally graded nano-scale films”, *Finite Elem. Anal. Des.*, **74**, 41-52.
- Shaat, M. and Mohamed, S.A. (2014), “Nonlinear-electrostatic analysis of micro-actuated beams based on couple stress and surface elasticity theories”, *Int. J. Mech. Sci.*, **84**, 208-217.
- Shaat, M., Mahmoud, F.F., Gao, X.L. and Faheem, A.F. (2014), “Size-dependent bending analysis of Kirchhoff nano-plates based on a modified couple-stress theory including surface effects”, *Int. J. Mech. Sci.*, **79**, 31-37.
- Thai, H.T. and Choi, D.H. (2013), “Size-dependent functionally graded Kirchhoff and Mindlin plate models based on a modified couple stress theory”, *Compos. Struct.*, **95**, 142-153.
- Toupin, R.A. (1962), “Elastic materials with couple-stresses”, *Arch. Rational Mech. Anal.*, **11**, 385-414.
- Tsiatas, G.C. (2009), “A new Kirchhoff plate model based on a modified couple stress theory”, *Int. J. Solid. Struct.*, **46**(13), 2757-64.
- Wang, Z.Q. and Zhao, Y.P. (2009), “Self-instability and bending behaviors of nano plates”, *Acta Mechanica Solida Sinica*, **22**(6), 630-643.
- Wang, Z.Q. and Zhao, Y.P. (2011), “Thermo-hyperelastic models for nanostructured materials”, *Sci. China: Phys. Mech. Astron.*, **54**, 948-956.
- Wang, Z.Q., Zhao, Y.P. and Huang, Z.P. (2010), “The effects of surface tension on the elastic properties of nano structures”, *Int. J. Eng. Sci.*, **48**, 140-150.
- Yaghoobi, H. and Fereidoon, A. (2010), “Influence of neutral surface position on deflection of functionally graded beam under uniformly distributed load”, *World Appl. Sci. J.*, **10**(3), 337-341.
- Yang, F., Chong, A.C.M., Lam, D.C.C. and Tong, P. (2002), “Couple stress based strain gradient theory for elasticity”, *Int. J. Solid. Struct.*, **39**(10), 2731-43.
- Yin, L., Qian, Q., Wang, L. and Xia, W. (2010), “Vibration analysis of microscale plates based on modified couple stress theory”, *Acta Mechanica Solida Sinica*, **23**(5), 386-93.

Appendix A

Since the plate is thin, the stress component σ_{zz} is small comparing to the in-plane stress components, which is simply assumed to be zero in the classical plate theory. However, due to surface tension a residual stress field will be developed in the bulk material; therefore it is assumed here that the stress component σ_{zz} varies linearly through the pate thickness (Lu *et al.* 2006, Shaat *et al.* 2012, 2013b, c, Lü *et al.* 2009). With the assumption, σ_{zz} can be written as

$$\sigma_{zz} = 0.5 (\tau_{\beta z, \beta}^+ - \tau_{\beta z, \beta}^-) + \frac{z + h_0}{h} (\tau_{\beta z, \beta}^+ + \tau_{\beta z, \beta}^-) \quad (A. 1)$$

Consequently, the symmetric force-stress tensor for the bulk with residual stresses, due to surface tension, can be written as follows

$$\sigma_{i\beta} = \lambda \varepsilon_{\gamma\gamma} \delta_{i\beta} + 2\mu \varepsilon_{i\beta} + \frac{\nu}{1-\nu} \sigma_{zz} \delta_{i\beta} \quad (A. 2)$$

From Eq. (14) and Eq. (15) in Eq. (7), then Eq. (A. 1) and then in Eq. (A. 2), the components of the force-stress tensor, for Mindlin plate, could be obtained

$$\begin{aligned} \sigma_{xx}^* &= \frac{\lambda(z)}{\nu} (u_{0,x} + \nu v_{0,y}) + \frac{(z + h_0)\lambda(z)}{\nu} (\phi_{x,x} + \nu \phi_{y,y}) \\ &+ \left(\frac{\nu}{(1-\nu)} \left(\frac{2\bar{\tau}_0(z + h_0)}{h} + \frac{\Delta\tau_0}{2} \right) \right) (\omega_{0,xx} + \omega_{0,yy}) \\ \sigma_{yy}^* &= \frac{\lambda(z)}{\nu} (v_{0,y} + \nu u_{0,x}) + \frac{(z + h_0)\lambda(z)}{\nu} (\phi_{y,y} + \nu \phi_{x,x}) \\ &+ \left(\frac{\nu}{(1-\nu)} \left(\frac{2\bar{\tau}_0(z + h_0)}{h} + \frac{\Delta\tau_0}{2} \right) \right) (\omega_{0,xx} + \omega_{0,yy}) \\ \sigma_{xy}^* &= \mu(z)(u_{0,y} + v_{0,x}) + (z + h_0)\mu(z)(\phi_{y,x} + \phi_{x,y}) \\ \sigma_{xz}^* &= K\mu(z)(\omega_{0,x} + \phi_x) \\ \sigma_{yz}^* &= K\mu(z)(\omega_{0,y} + \phi_y) \end{aligned} \quad (A. 3)$$

where $\lambda(z) = \frac{\nu E(z)}{1-\nu^2}$ and $\mu(z) = \frac{E(z)}{2(1+\nu)}$ are FG plate bulk Lamé constants. Moreover, From Eq. (17) in Eq. (5b), the symmetric couple-stress tensor m_{ij} , for Mindlin plate, can be obtained

$$\begin{aligned} m_{xx} &= \mu(z)\ell(z)^2(\omega_{0,xy} - \phi_{y,x}) \\ m_{yy} &= \mu(z)\ell(z)^2(\phi_{x,y} - \omega_{0,xy}) \\ m_{zz} &= \mu(z)\ell(z)^2(\phi_{y,x} - \phi_{x,y}) \\ m_{xy} &= \frac{\mu(z)\ell(z)^2}{2} (\omega_{0,yy} - \omega_{0,xx} + \phi_{x,x} - \phi_{y,y}) \\ m_{xz} &= \frac{\mu(z)\ell(z)^2}{4} \left((v_{0,xx} - u_{0,xy}) + (z + h_0)(\phi_{y,xx} - \phi_{x,xy}) \right) \\ m_{yz} &= \frac{\mu(z)\ell(z)^2}{4} \left((v_{0,xy} - u_{0,yy}) + (z + h_0)(\phi_{y,xy} - \phi_{x,yy}) \right) \end{aligned} \quad (A. 4)$$

The stress resultants $N_{ij}^*, M_{\alpha\beta}^*, P_{ij}$ and $R_{\alpha z}$ for Mindlin plate theory can be obtained by substituting the displacement fields (Eq.(14)) into Eq. (7), Eq.(A.3)and Eq. (A. 4) and then into Eq. (19) and Eq. (20).

$$\begin{aligned}
N_{xx}^* &= 4\bar{\tau}_0 + A_{11}^*u_{0,x} + A_{12}^*v_{0,y} + B_{11}^*\phi_{x,x} + B_{12}^*\phi_{y,y} + \left(\frac{\Delta\tau_0 h v}{2(1-v)} + \frac{2v h_0 \bar{\tau}_0}{(1-v)}\right)(\omega_{0,xx} + \omega_{0,yy}), \\
N_{yy}^* &= 4\bar{\tau}_0 + A_{22}^*v_{0,y} + A_{12}^*u_{0,x} + B_{22}^*\phi_{y,y} + B_{12}^*\phi_{x,x} + \left(\frac{\Delta\tau_0 h v}{2(1-v)} + \frac{2v h_0 \bar{\tau}_0}{(1-v)}\right)(\omega_{0,xx} + \omega_{0,yy}), \\
N_{xy}^* &= 4\bar{\tau}_0 + A_{66}^*(u_{0,y} + v_{0,x}) + B_{66}^*(\phi_{y,x} + \phi_{x,y}), \\
N_{xz}^* &= A_{44}(\omega_{0,x} + \phi_{x,x}) + 2\bar{\tau}_0\omega_{0,x}, \\
N_{yz}^* &= A_{55}(\omega_{0,y} + \phi_{y,y}) + 2\bar{\tau}_0\omega_{0,y}, \\
M_{xx}^* &= B_{11}^*u_{0,x} + B_{12}^*v_{0,y} + D_{11}^*\phi_{x,x} + D_{12}^*\phi_{y,y} \\
&+ \left(\frac{v(\bar{\tau}_0(h^2 + 12h_0^2) + (3\Delta\tau_0 h h_0))}{6(1-v)}\right)(\omega_{0,xx} + \omega_{0,yy}) + \Delta\tau_0 h, \\
M_{yy}^* &= B_{22}^*v_{0,y} + B_{12}^*u_{0,x} + D_{22}^*\phi_{y,y} + D_{12}^*\phi_{x,x} \\
&+ \left(\frac{v(\bar{\tau}_0(h^2 + 12h_0^2) + (3\Delta\tau_0 h h_0))}{6(1-v)}\right)(\omega_{0,xx} + \omega_{0,yy}) + \Delta\tau_0 h, \\
M_{xy}^* &= B_{66}^*(u_{0,y} + v_{0,x}) + D_{66}^*(\phi_{x,y} + \phi_{y,x}) + \Delta\tau_0 h
\end{aligned} \tag{A.5}$$

$$\begin{aligned}
P_{xx} &= A_n(\omega_{0,xy} - \phi_{y,x}) \\
P_{yy} &= A_n(\phi_{x,y} - \omega_{0,xy}) \\
P_{zz} &= A_n(\phi_{y,x} - \phi_{x,y}) \\
P_{xy} &= \frac{A_n}{2}(\omega_{0,yy} - \omega_{0,xx} + \phi_{x,x} - \phi_{y,y}) \\
P_{xz} &= \frac{A_n}{2}(v_{0,xx} - u_{0,xy}) + \frac{1}{2}(h_0 A_n + B_n)(\phi_{y,xx} - \phi_{x,xy}) \\
P_{yz} &= \frac{A_n}{2}(v_{0,xy} - u_{0,yy}) + \frac{1}{2}(h_0 A_n + B_n)(\phi_{y,xy} - \phi_{x,yy}) \\
R_{xz} &= \frac{1}{2}(h_0 A_n + B_n)(v_{0,xx} - u_{0,xy}) + \frac{1}{2}(h_0^2 A_n + 2B_n + D_n)(\phi_{y,xx} - \phi_{x,xy}) \\
R_{yz} &= \frac{1}{2}(h_0 A_n + B_n)(v_{0,xy} - u_{0,yy}) + \frac{1}{2}(h_0^2 A_n + 2B_n + D_n)(\phi_{y,xy} - \phi_{x,yy})
\end{aligned} \tag{A.6}$$